Journal of The Electrochemical Society, **160** (9) H630-H635 (2013)
0013-4651/2013/160(9)/H630/6/$31.00 © The Electrochemical Society

Electrical Properties of Two-Dimensional Gold Nanoparticle–Alkanethiol Networks Formed on Plastic Microbeads

Hiroshi Shiigi,[a,*,z] Shuji Shirai,[a] Takahiro Fujita,[a] Hisashi Morishita,[a] Yojiro Yamamoto,[a,b] Tomoaki Nishino,[c] Shiho Tokonami,[c] Hidenobu Nakao,[d] and Tsutomu Nagaoka[a,*]

[a]*Department of Applied Chemistry, Osaka Prefecture University, Sakai, Osaka 599-8570, Japan*
[b]*Green Chem. Inc., Sakai, Osaka 599-8241, Japan*
[c]*Nanoscience & Nanotechnology Research Center, Osaka Prefecture University, Sakai, Osaka 599-8570, Japan*
[d]*National Institute for Materials Science, Tsukuba, Ibaraki 305-0047, Japan*

It is the ultimate goal to accurately place molecules and spaces while building electronic devices using individual molecules. In this paper, we attempt to form a metal–insulator–metal (MIM) junction on micrometer-sized plastic beads that can be placed where desired. Electron tunneling in an MIM junction formed from a two-dimensional network consisting of repeated gold nanoparticle (AuNP)–alkyl chain–AuNP sequences is evaluated by directly measuring the electrical resistivity of the microbead. A plot of the logarithm of the resistivity versus the number of carbon atoms in the alkyl chain ($n_c = 3$–8) in each junction yields identical tunneling coefficients, β, of 8.59 ± 0.09 nm^{-1}. The MIM junction on a microbead can be moved and arranged in any location, which enables the rapid development of miniaturized compact electronic devices.
 [DOI: 10.1149/2.110309jes]

Manuscript submitted June 3, 2013; revised manuscript received July 9, 2013. Published July 17, 2013.

New strategies that involve a combination of nanomaterials and nanofabrication techniques have been developed in the field of nano- and micro-electronics. Information technology and related fields have undergone rapid progress and development; this has made it necessary to miniaturize compact electronic devices and consumer electronic products, such as mobile phones, personal digital assistants, and laptops through high-density packaging and wiring technologies. For further development, wires, switches, and sensor-like devices that use various techniques to control the electron or charge transport in molecules have been studied intensively as new technologies for the generation beyond the recent rapid developments.[1–6] Although building an electronic device using individual molecules is one of the ultimate goals in nanotechnology, it is also very important to determine where and how to place functional molecules and spaces.

Recently, inorganic nanoparticles (NPs) and their arrays have attracted the attention of researchers as important materials for nano- and micro-electronics owing to their unique physical and chemical properties.[7–10] Self-assembly technology can be effectively used to assemble well-organized one- to three-dimensional structures, and interparticle connections can be controlled at the single-particle level.[5,11–15] Metal NPs are one of the most frequently studied inorganic materials for applications in various nanotechnology-oriented devices;[16–18] their distinct combinations can impart unique functionality to devices.[19,20] We previously reported gold NP (AuNP) arrays that were prepared via a single-step procedure using self-assembling alkanethiols to deposit AuNPs on a planer plastic substrate.[21–23]

A well-studied molecular system is the alkyl chain, which consists of saturated C–C bonds terminated by linkers that can bind to electrodes to form metal–insulator–metal (MIM) junctions.[6,24–34] Alkyl chains have a large gap between the highest occupied (HOMO) and lowest unoccupied (LUMO) molecular orbitals, resulting in poor conductivity. A number of experiments have revealed that the conductivity and resistance of the alkyl moiety decreases and increases, respectively, exponentially with increasing molecular length. The exponential decay together with characteristic current–voltage curves and temperature independence suggest electron tunneling as the mechanism for conduction through the molecules. Therefore, the MIM junction is a potential component of memory and logic elements in molecular electronics. Although MIM junctions obtained between mercury droplets and metals (i.e., Hg or Ag),[24–28] and/or gold-coated tips for the scanning probe microscope (SPM) and gold substrates[29–34] revealed electrical characteristics based on electron tunneling through the molecules, the constrained freedom of the arrangement of the junctions limited their applications.

Herein, we report the straightforward formation of an MIM junction using AuNPs and alkanethiol moieties on a plastic microbead. The plastic microbeads are generally coated with metals and act as cores for conducting spacers. The conducting microbead is compressed to form the connections between the input/output connections and external circuit via a single installation procedure for consumer electronic products through high-density packaging. To use as an electrical connection in the high-density packaging, it is required conventionally that high electrical conductivity and high environmental stability are applied to the microbeads. It becomes possible to control the electrical properties of the beads, we can form micrometer-sized electric circuits desired by an arrangement and combination of the beads and apply them to electronic devices. Since the formation of the MIM junction on a core plastic microbead enables movement and arrangement of the MIM junction at a specific location, these molecular electronics can be applied to the rapid development of miniaturized compact electronic devices and consumer electronic products through high-density packaging and wiring technologies.

Experimental

Chemicals.— All the chemicals used were of reagent grade. Ultrapure water (>18 MΩ cm), after ultraviolet sterilization, was used throughout the experiment. Chloroauric acid and sodium citrate, which were used to prepare gold nanoparticle (AuNP), and alkanethiols, which was used as binders, were purchased from Wako Pure Chemical Industries. Acrylic resin microbead with a mean diameter of 5 μm (M-11, Hayakawa Rubber) were used as a substrate.

Preparation of 30 nm AuNP.— In this study, AuNP was prepared by the conventional chemical reduction method in an aqueous solution.[16,17,21] AuNP used here was prepared by a reduction of aqueous $HAuCl_4$ with sodium citrate, as follows. A 24 mL aliquot of 1 wt% $HAuCl_4$ was added to 179 mL of 0.26 wt% sodium citrate and stirred at 80°C for 20 min. Characterization using a zeta-potential & particle size analyzer (ELSZ-2Plus, Otsuka Electronics) revealed that the AuNP produced had a mean diameter of 30.8 ± 4.0 nm.

Formation of two-dimensional (2D) networks consisting of AuNPs on plastic microbeads.— The AuNPs were deposited on a plastic microbead in a single step, as shown in Scheme 1.[35–37] Fifty mg of acrylic resin microbead with a mean diameter of 5 μm and alkanethiol ($C_nH_{2n+1}SH$), as a binder, were added to the colloidal gold dispersion (33.3 mL); the mixture was then stirred at room temperature for one day. The thiol group (SH) of the alkanethiol molecules adsorbed onto the AuNP surface through chemisorption, whereas the

*Electrochemical Society Active Member.
zE-mail: shii@chem.osakafu-u.ac.jp

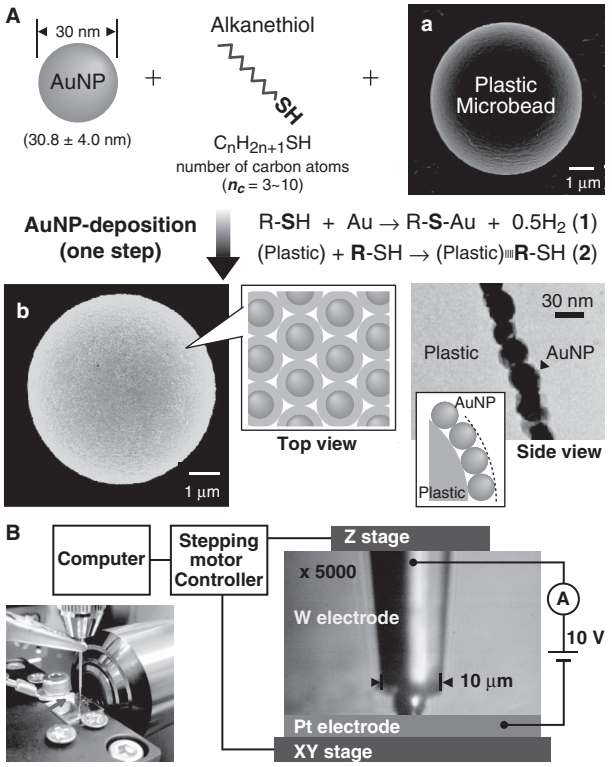

Scheme 1. Schematics of (A) one-step preparation procedure and (B) electrical evaluation of a AuNP-coated microbead. SEM images of (a) an uncoated microbead and (b) a AuNP-covered microbead along with a cross-section TEM image.

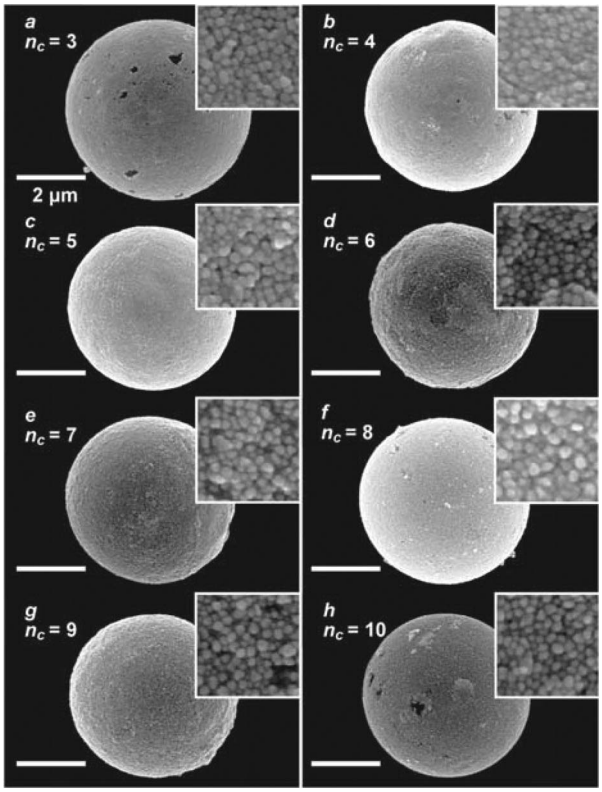

Figure 1. SEM images of AuNP-coated microbeads prepared using various alkanethiols: (a) propane-, (b) butane-, (c) pentane-, (d) hexane-, (e) heptane-, (f) octane-, (g) nonane-, and (h) decanethiol. The number of carbon atoms in the alkanethiol is represented by n_c. The scale bar is 2 μm.

alkyl chains bound to the plastic surface through hydrophobic interactions in aqueous solution (Eqs. 1 and 2 in Scheme 1(A)). Alkanethiols such as propane, butane, heptane, hexane, pentane, octane, nonane, and decanethiol were used as binders. The amount of thiol added to the AuNP dispersion was optimized in Table I.[35] The number of carbon atoms in the alkyl chain is represented as n_c. Molecular length of alkanethiols was calculated with a MOPAC ver.3.9.0. After the AuNP-coated microbeads were separated via filtration, they were washed with an ample amount of water and dried in vacuo. The surfaces of the microbeads were imaged using field-emission scanning electron microscopy (FE-SEM; S-4700, Hitachi) at an applied voltage of 10 kV.

Electrical evaluation of the AuNP-coated microbeads.— The electrical characteristics of a single microbead were directly measured using a digital ultra-high-resistance meter (8340A, ADCMT) that monitored the current between 1 fA and 20 mA at a constant voltage (10 V) in an air-conditioned room (25 ± 1°C).[35–37] The laboratory-made probe setup comprised a Pt plate (1 × 1 cm) and an electrochemically polished tungsten tip (10 μm in diameter) that served as the common ground and movable electrode, respectively, as shown in Scheme 1(B). During the measurements, a single microbead was compressed 10–60% between the W probe tip and Pt plate; the compression was calculated from the movement on the Z-axis, as controlled with the stepping motor. The measurement was carried out on at least ten beads to obtain an average value.

Table I. Preparation condition of AuNP-coated beads.

Alkanethiol (n_c)	Molecular length (nm)	Amount (μmol)
Butanethiol (4)	0.62	17.5
Pentanethiol (5)	0.75	12.1
Hexanethiol (6)	0.88	7.46
Heptanethiol (7)	1.00	5.86
Octanethiol (8)	1.14	4.03
Nonanethiol (9)	1.26	3.15
Decanethiol (10)	1.40	2.23

Thermogravimetric analysis to determine the ability of alkanethiol to bind AuNPs to microbeads.— The desorption temperatures of alkanethiol from AuNPs, a microbead, and a AuNP-covered microbead were estimated using thermogravimetry-differential thermal analysis/mass spectrometry (TG-DTA/MS; 9600 series, Bruker AXS) under a 99.9999% helium atmosphere. The temperature was increased from room temperature (~20°C) to 300°C at a programmed heating rate of 5°C min^{-1}. Samples (10 mg) were dried in a vacuum overnight and transferred to a Pt holder.[37] TG measurements of the simple alkanethiols were carried out on a 10 μL droplet at a heating rate of 2°C min^{-1}.

Results and Discussion

SEM observation of a 2D network formed on a microbead.— SEM images of the AuNP-coated microbeads are shown in Figure 1: A uniformly covered surface is observed for all alkanethiols. Overlap of the AuNPs was not evident, although bare portions of microbead surface that did not have an adsorbed layer of AuNPs were present. These results indicate that a single layer of AuNPs formed on the plastic microbead without aggregation or integration.

Thermal characteristics of the 2D network on a microbead.— Thermogravimetric analysis of the AuNP-coated microbeads revealed the role of alkanethiol in the formation of a single layer of AuNPs. During the TG analysis of decanethiol, a large weight loss was observed at 120°C and fragmentation of the molecule at 120°C was evident, as

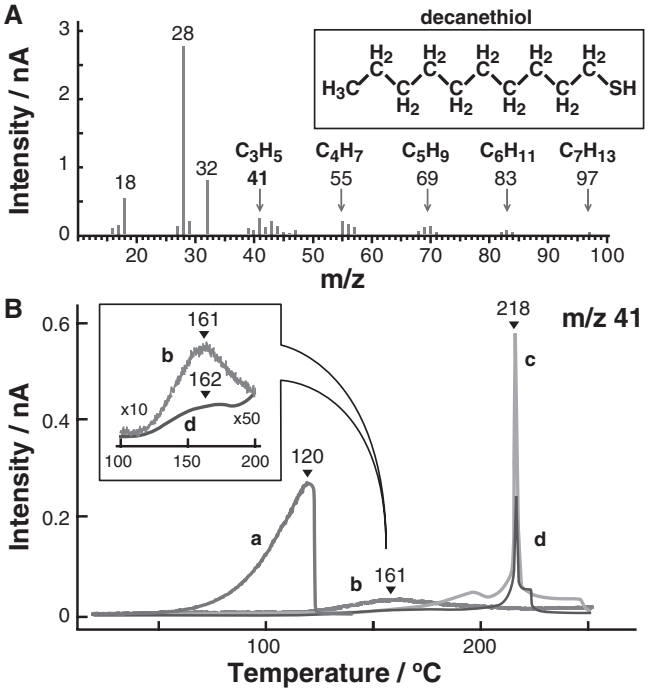

Figure 2. (A) Fragment pattern vs. mass number (m/z) of decanethiol at 120°C. (B) Temperature profile of m/z 41. Profiles of (a) decanethiol, (b) decanethiol-modified microbeads, (c) decanethiol-coated AuNPs, and (d) AuNP-coated microbeads. The inset is an enlarged view of profiles (b) and (d) from 100 to 200°C.

shown in Figure 2A. Peaks observed at mass numbers (m/z values) of 41, 55, 69, and 83, are attributed to the C_3H_5, C_4H_7, C_5H_9, and C_6H_{11} fragments, respectively, of the alkyl chain. In addition, peaks attributed to atmospheric gases, i.e., H_2O (m/z 18), N_2 (28), and O_2 (32) were evident throughout the temperature range.[38] The peak at m/z 41, which is attributed to the C_3H_5 fragment, was the most intense peak in the fragment pattern of decanethiol, and was not affected by other fragments below 300°C. Since a peak for the C_3H_5 fragment appeared for all of the alkanethiols, desorption temperature was investigated by focusing on the peak at m/z 41, as listed in Table II. An intense peak was observed at 120°C in the temperature profile of decanethiol, whereas the profile of the decanethiol-modified microbeads features a broad peak at 161°C, as shown in Figure 2B. Similarly, a broad peak at 162°C was observed in the profile of AuNP-covered microbeads, as shown in the inset of Figure 2B(d). These results indicate that decanethiol interacts with the surface of the plastic microbead, which agrees with the results of a previous report.[21,22] We previously reported that the adsorption of butanethiol to a polystyrene substrate increased the surface roughness, which was confirmed via SPM observations. The results revealed that the alkyl chains adsorb

Table II. Desorption temperature of alkanethiol based on the number of carbon atoms in the alkanethiol (n_c).

	Temperature (°C)			
n_c	Alkanethiol	Binder/bead	Binder/AuNP	AuNP/binder/bead
3	22.4	120	170	123, 169
4	30.1	123	196	125, 197
5	32.7	135	208	135, 207
6	48.9	145	213	143, 217
7	76.6	155	214	154, 217
8	91.4	156	216	155, 218
9	108	158	218	159, 220
10	120	161	217	162, 217

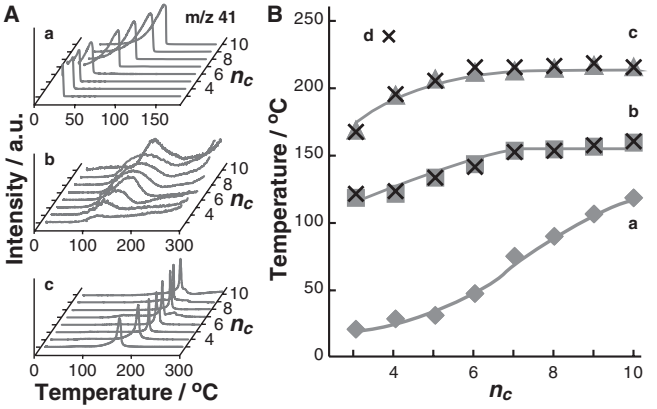

Figure 3. (A) Temperature profiles of m/z 41 for (a) alkanethiol, (b) alkanethiol-modified microbeads, and (c) alkanethiol-coated AuNPs. (B) Dependence of the peak temperature in the profile on the n_c of (a) alkanethiol, (b) alkanethiol-modified microbeads, (c) alkanethiol-coated AuNPs and (d) AuNP-coated microbeads.

to the surface of the substrate via hydrophobic interactions (Eqs. 1 and 2 in Scheme 1(A)) because they do not have appropriate functional groups for binding with each other beside the SH group. Desorption of decanethiol from the plastic microbead and AuNP-coated microbead (Figures 2B(b) and (d)) was observed at a higher temperature than that of simple decanethiol: The peak shifted from 120 to 160°C, which is due to the hydrophobic interactions between the alkyl chains and plastic surface. Since there are no peaks in the lower temperature region in these profiles, all decanethiol interacts with the surface of the microbead, i.e., there is no free alkanethiol. Peaks were observed at 218°C for decanethiol-coated AuNPs and AuNP-coated microbeads (Figures 2B(c) and (d)). The larger peak shift, as compared to that based on the hydrophobic interactions, is attributed to cleavage of the Au–S bonds.[39–41] It is difficult to determine the reaction rates of alkanethiol binding to AuNPs and microbeads; however, this data suggests that the force binding alkanethiol to the AuNPs (i.e., the Au–S bond) is stronger than the hydrophobic interactions between alkanethiol and microbead. The desorption of decanethiol from the microbead (161°C) and AuNPs (218°C) was observed at higher temperatures than that of simple decanethiol (120°C) since decanethiol forms a chemical bond and/or interacts with the AuNPs and microbeads. Therefore, decanethiol plays an important role as a binder for AuNP deposition on microbeads.

Since interesting results were obtained by focusing on the C_3H_5 fragment, which was the most intense peak in the fragment pattern of the thiols used, temperature profiles of alkanethiols, alkanethiol-modified microbeads, and alkanethiol-coated AuNPs were obtained by monitoring m/z 41; these profiles are shown in Figures 3A. Although the TG curve of propanethiol ($n_c = 3$) was difficult to obtain due to its high volatility, its profile has a clear peak around room temperature (22.4°C). The peak dramatically shifts to higher temperatures with increasing n_c, as shown in Figure 3A(a). On the other hand, desorption of propanethiol from the microbeads and AuNPs was observed above 100°C (Figure 3A(b) and (c)). The profile of the AuNP-coated microbeads features peaks at 123 and 169°C; these peak temperatures correlate closely with the desorption temperatures of propanethiol from microbeads (120°C) and AuNPs (170°C), respectively. In the same manner, two peaks observed in the profiles of AuNP-coated microbeads were in good agreement with the desorption temperature of the corresponding alkanethiol from microbeads and AuNPs (Table II). Therefore, the role of alkanethiol as a binder for the formation of AuNP-coated microbeads was clarified by focusing on the desorption of alkanethiol from microbeads and AuNPs. The peak temperature monotonically increased with increasing n_c, as shown in Figure 3B(a). Similarly, the temperature of the desorption of alkanethiol from microbeads increased with increasing n_c,

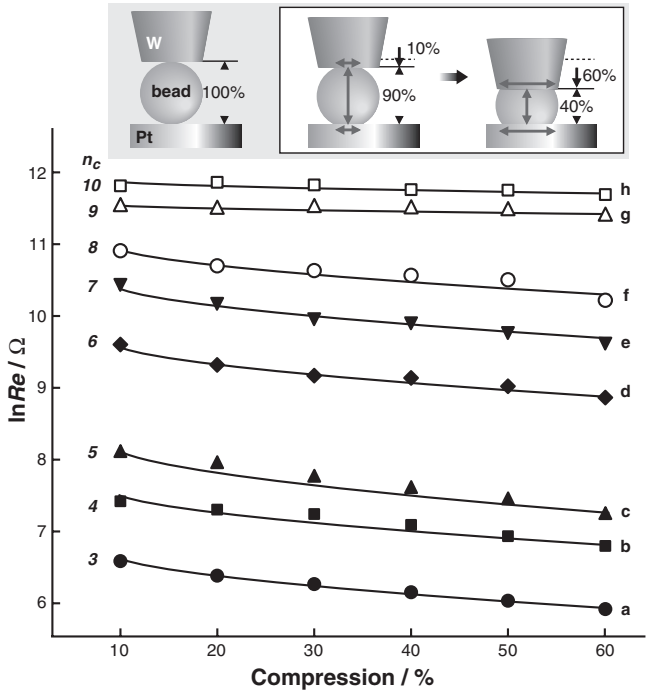

Figure 4. Dependence of the ln(*Re*) of the AuNP-coated microbead on the compression from 10 to 60% for alkanethiols with n_c values of (a) 3, (b) 4, (c) 5, (d) 6, (e) 7, (f) 8, (g) 9, and (h) 10. The upper detection limit of the instrument is 100 T Ω. The compression, which was controlled by a stepping motor, was calculated from the movement in the Z-axis direction.

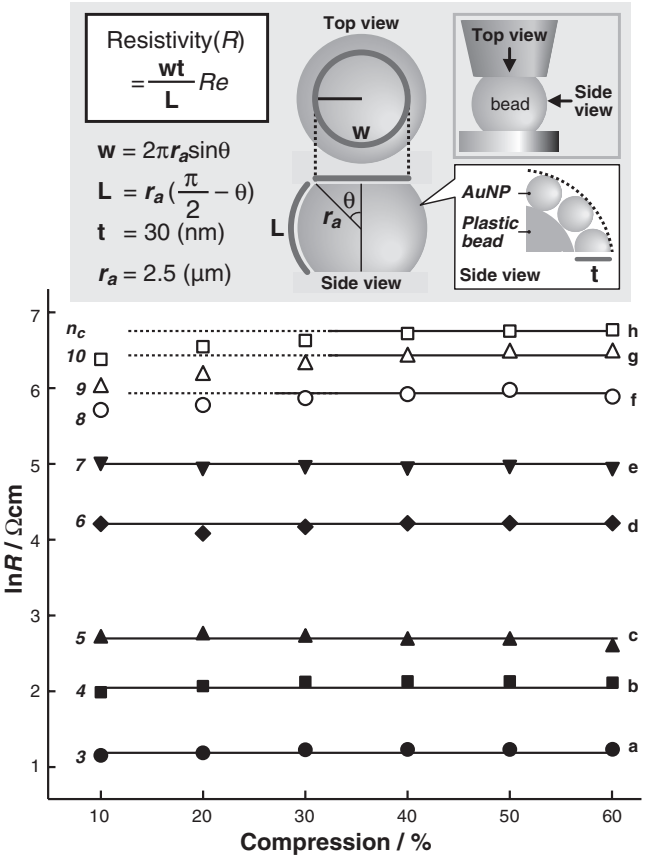

Figure 5. Dependence of the ln(*R*) of the AuNP-coated microbead on the compression from 10 to 60% for alkanethiols with n_c values of (a) 3, (b) 4, (c) 5, (d) 6, (e) 7, (f) 8, (g) 9, and (h) 10. The upper detection limit of the instrument is 10^9 Ω cm. The inset defines a calculation of the resistivity of a single microbead. L: length, w: width, t: thickness (= 30 nm; a mean diameter of AuNP), r_a: a radius of microbead (= 2.5 μm).

but remained constant at an n_c value of 7 (b) (*refer to* Table II). The temperature depends on the energy required for a desorption of the alkanethiol from the microbead. We cannot make detailed quantitative or qualitative discussions about the desorption energy from only these results, because it is based on some interactions working in the alkanethiol on the bead and between the beads and the alkanethiol. Moreover, this plot has a large y-intercept of ∼100°C, which is due to the hydrophobic interactions between the alkyl chains and the plastic surface of the microbeads. The hydrophobic interactions strengthen with increasing n_c, as mentioned above. Since there no peaks are evident in the lower temperature region of all profiles (refer to Figure 3A(b)), all alkanethiols, even those with short alkyl chains, interact with the surface of the microbead. Similarly, the desorption temperature of alkanethiol from AuNPs also increased with increasing n_c (c), and the temperature profile has a y-intercept greater than 100°C. Previous reports revealed that the desorption of thiols from AuNP via Au–S bond breakage were observed around 150–300°C; the enthalpies of the bonds were estimated to be ∼115–140 kcal mol^{-1}.[42,43] Therefore, it is expected that the y-intercept of the plot of the alkanethiol-covered AuNPs would be at least 150°C.[44–46] These data imply that the alkanethiol adsorbed onto the AuNPs through Au–S bonds; furthermore, van der Waals interactions existed between adjacent alkanethiols on the surface of AuNPs. Therefore, the desorption temperature increased with increasing length of alkyl chains due to the increasing van der Waals interactions. In other words, longer alkanethiols lead to stronger adhesion between the AuNPs and microbead. However, the desorption temperature of thiols from AuNPs became constant at 218°C over an n_c value of 8. This is consistent with the temperatures reported for a dodecanethiol-coated AuNP (190°C) and an octanethiol-coated Au cluster (230°C).[47,48] Accordingly, using alkanethiol as a binder afforded not only stronger adhesion between the AuNPs and microbead in the vertical direction, but also between adjacent AuNPs in the horizontal direction.

Considering these results together with the SEM observations, AuNP deposition using alkanethiol results in the formation of a 2D network consisting of repeated AuNP–alkanethiol–AuNP sequences on plastic microbeads.

Electrical properties of the 2D network on a microbead.— Figure 4 shows the dependence of the logarithmic electrical resistance (*Re*) of the AuNP-coated microbeads on the compression (10–60%). In the curves (a–f), the ln(*Re*) decreases gradually with increasing compression rate. In contrast, the curves (g) and (h) feature a slightly decrease of ln(*Re*) with increasing compression rate. The decrease in the ln(*Re*) is attributed to an increase in the contact area between the electrodes (i.e., the W tip and Pt plate) and microbead, and a decrease in the distance through the microbead between the electrodes with increasing compression rate as shown in the inset of Figure 4. It seems that the y-intercepts, ln(Re_0), depend on the length of the alkyl chain. Therefore, a slight decrease of ln(*Re*) observed in the curves (g, h) has been greatly contributed by the interfacial resistance rather than that of the 2D network on the microbead. These imply that the resistance of the microbead are reflected by the resistivity of the 2D network on the microbead and the interfacial resistance between the electrodes and microbead.

To estimate their contributions, the resistivity (*R*) was calculated according to a formula shown in the inset of Figure 5. Figure 5 shows the dependence of the logarithmic resistivity (*R*) of the AuNP-coated microbeads on the compression (10–60%). In the curves (a–e), there is no change in ln(*R*) with increasing compression rate. The y-intercepts, ln($R_{0\%}$), which clearly depend on the length of the alkyl chain, are reflected by interfacial resistance between the electrodes and microbead. These indicate that the resistivity of the 2D network on the microbead

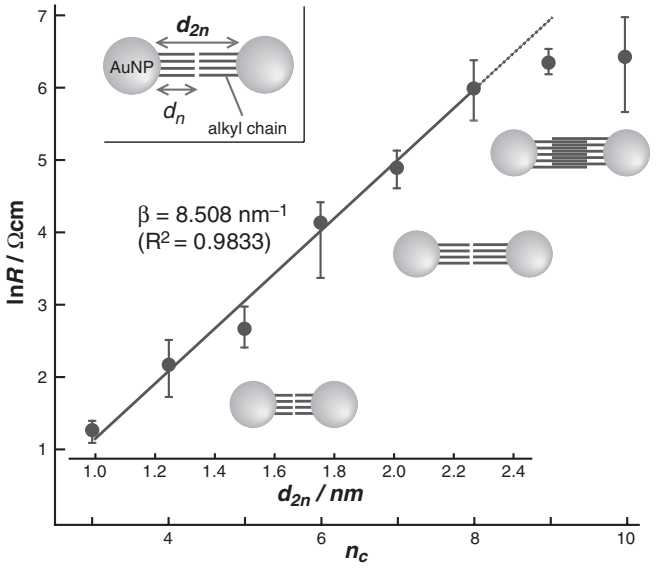

Figure 6. Dependence of the ln(R) of the AuNP-coated microbead at 40% compression on n_c. The measurements were performed on at least ten microbeads to obtain an average value. The value of β was obtained from the slope of the fitting curve. The inset represents a model of the gap (d_{2n}) formed between adjacent AuNPs.

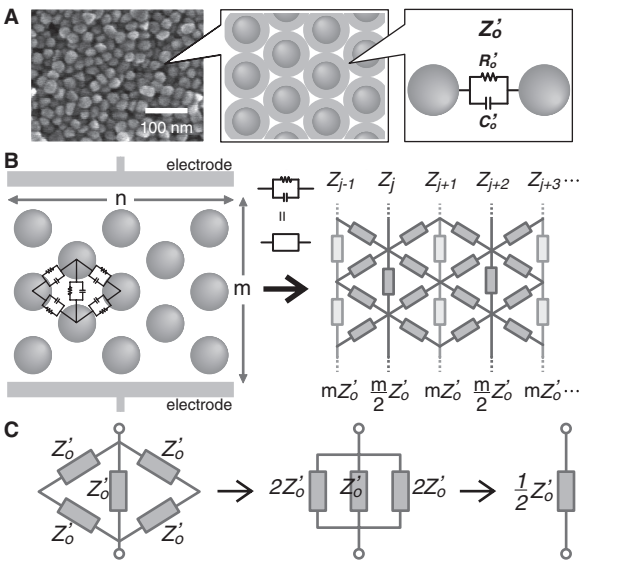

Scheme 2. Illustration of the 2D network on a plastic microbead. (A) Illustration of the 2D network derived from SEM images and a model of the electrical equivalent (Z'_0) between adjacent AuNPs expressed as a capacitor (C'_0) and resistor (R'_0), (B) 2D network consisting of a parallel RC circuit model (m, n are independent positive integers), and (C) calculation process for the derivation of equation 1.

dominates the ln(R) at n_c values less than 8. In contrast, the curves (f–h) feature a slightly increase of ln(R) with increasing compression rate until it becomes constant over 40%. This implies that the longer alkyl chain ($n_c > 8$) behaves as an uncertainty for electrical measurement and significantly affects the resistivity at compressions less than 40%. It is notable that there is a connection through the alkanethiol molecules at the interface of the electrodes and AuNPs on the microbead. Therefore, the ln(R) of the AuNP-coated microbead depends not only on the resistivity of the 2D network, but also the uncertainty, which is based on the size of the alkyl chain at n_c values greater than 8. In other words, larger alkanethiol moieties between the electrodes and the microbead significantly contribute to the resistivity. The contribution of an uncertainty is almost negligible over 40% compressions.

A plot of ln(R) vs. the gap between AuNPs (d_{2n}) was obtained at 40% compression to ensure a reliable contact and minimize the uncertainty, as shown in Figure 6. The R of the AuNP-coated microbead exponentially increases with increasing n_c. This phenomenon is attributed to the predominant mechanism of electron transport through a self-assembled monolayer (SAM) in MIM junctions.[24–28,49,50] A number of studies have concluded that the electrical properties of the junction through a SAM between electrodes can be determined by considering it as a parallel circuit composed of a resistor and capacitor.[51–53]

Since each AuNP is separated from the other AuNPs by alkanethiols, adjacent AuNPs electrically act as capacitors and resistors, as shown in Scheme 2(A).[53] Consequently, the electrical equivalent (Z'_0) of the two particles can also be expressed as a resistor (R'_0) and capacitor (C'_0) connected in parallel, and the whole network (Z_{total}) can be considered as a parallel circuit composed of a resistor and capacitor (see Scheme 2(B) and 2(C)):

$$Z_{total} = \left(\frac{2m}{3n}\right) Z'_0 \quad (m,\ n = \text{positive integer}) \qquad [1]$$

This circuit scheme is supported by the Cole-Cole plot of a single hemisphere and from the excellent agreement between the DC and AC resistance measurements.[23] Therefore, it can be understand easily that a distance between the adjacent AuNPs dominates the electrical characteristics of the 2D network formed by depositing AuNPs on a microbead. In other words, it is possible to evaluate the electrical property of the AuNP-coated microbead by focusing on the length of the alkanethiol in a pair of AuNPs as a model in the Figure 6.

Electron transport in the AuNP–alkyl chain–alkyl chain–AuNP junction is dominated by the tunneling barrier, i.e., resistivity, at a constant applied voltage of 10 V, which decays exponentially with the junction distance according to the following equation:

$$\ln(R_0/R) = -\beta d_{2n} \qquad [2]$$

where β is the decay constant, which reflects the strength of electronic coupling across a particular molecular bridge (tunneling coefficient), and d_{2n} is twice the length of the alkanethiol (d_n) along the tunneling pathway. The slope of 8.51 nm^{-1} that was obtained from the approximate curve of the plot of ln(R) vs. d_{2n}, which has a y-intercept of ln(R_0), was consistent with the value of β reported for tunneling through alkanethiols.[24–28,51–57] However, the ln(R) of the AuNP-coated microbead deviated from the linear plot at n_c values greater than 8 (i.e., $d_{2n} = 2.27$ nm) and reached a constant value of ~10^6 Ω cm. This indicates that alkyl chains bound to the surfaces of adjacent AuNPs interacted more strongly and become more interdigitated as their length increased while shorter binders had weaker interactions and did not interdigitate.[58]

The values of β obtained from plots of the ln(R) vs. d_{2n} at n_c values less than 8 for the AuNP-coated microbeads at compressions of 10 to 60% were almost identical, as shown in Table III. The y-intercepts, ln(R_0), of the approximate curves, which are based on the contact

Table III. Values of β for AuNP–alkyl chain–alkyl chain–AuNP junctions on a bead with compression.

Compression (%)	β (nm^{-1})	ln(R_0) (mΩ cm)	R^2
0	8.601	2.87	0.9848
10	8.694	2.58	0.9855
20	8.642	2.66	0.9907
30	8.562	3.16	0.9872
40	8.508	3.34	0.9833
50	8.573	3.03	0.9801
60	8.577	2.96	0.9716

resistance, are almost identical and negligibly small (∼3 mΩ cm). Moreover, a plot of the interfacial resistance, ln($R_{0\%}$), which was obtained as y-intercepts in Figure 5 vs. d_{2n} indicated a linear relationship with a slope of ∼8.60 nm^{-1} ($r = 0\%$). This indicates that the interfacial resistance is also based on twice the length of the alkyl chain (d_{2n}) at the interface of the electrodes (the W tip and Pt plate) and AuNPs on the microbead. Therefore, the d_{2n} is independent of the compression and dominates the resistivity of the 2D network on the microbead.

It is concluded that the electrical results are based on electron transfers in the 2D network that occur by tunneling through binders between adjacent AuNPs. Therefore, precise control of the nanogap between adjacent AuNPs is achieved based on the number of carbon atoms in the alkyl chain; in particular, shorter alkanethiols ($n_c = 3$–8) enable molecular level control at between 0.98 and 2.3 nm without interdigitation.

Conclusions

A molecular junction consisting of repeated AuNP–alkyl chain–alkyl chain–AuNP sequences was formed as a 2D network on a microbead. Electrical evaluation of the junction revealed tunneling coefficients ($\beta = 8.59 \pm 0.09$ nm^{-1}) identical to those obtained in previous works using special instruments; i.e., Hg dropping system and SPM. Microbeads are generally coated with metals and used as cores for conducting spacers. The conducting microbead is compressed to form the connections between the input/output and external circuit via a single installation procedure in consumer electronic products through high-density packaging. Therefore, the MIM junction on a microbead enables the movement and arrangement of the junction in any location and the application of molecular electronics to the rapid development of miniaturized compact electronic devices through high-density packaging. It is also expected that the AuNPs separated on the microbead provides a significant advantage in optical applications due to the surface or localized surface plasmon resonances.

Acknowledgment

We gratefully acknowledge the financial support provided by the Japan Society for the Promotion of Science through a grant-in-Aid for Scientific Research (B) (JSPS KAKENHI, 25288039).

References

1. M. A. Reed, C. Zhou, C. J. Muller, T. P. Burgin, and J. M. Tour, *Science*, **278**, 252 (1997).
2. S. J. Tans, A. R. M. Verschueren, and C. Dekker, *Nature*, **393**, 49 (1998).
3. D. Porath, A. Bezryadin, S. de Vries, and C. Dekker, *Nature*, **403**, 635 (2000).
4. W. Liang, M. P. Shores, M. Bockrath, J. R. Long, and H. Park, *Nature*, **417**, 725 (2002).
5. H. Nakao, H. Shiigi, Y. Yamamoto, S. Tokonami, T. Nagaoka, S. Sugiyama, and T. Ohtani, *Nano Lett.*, **3**, 1391 (2003).
6. N. Tao, *Nat. Nano.*, **1**, 173 (2006).
7. L. Li, J. Hu, W. Yang, and A. P. Alivisatos, *Nano Lett.*, **1**, 349 (2001).
8. C. A. Foss, G. L. Hornyak, J. A. Stockert, and C. R. Martin, *J. Phys. Chem.*, **98**, 2963 (1994).
9. K. Yakushiji, F. Ernult, H. Imamura, K. Yamane, S. Mitani, K. Takanashi, S. Takahashi, S. Maekawa, and H. Fujimori, *Nat. Mater.*, **4**, 57 (2005).
10. Y. Azuma, M. Kanehara, T. Teranishi, and Y. Majima, *Phys. Rev. Lett.*, **96**, 016108 (2006).
11. H. Shiigi, Y. Yamamoto, N. Yoshi, H. Nakao, and T. Nagaoka, *Chem. Commun.*, **2006**, 4288.
12. H. Shiigi, R. Morita, Y. Yamamoto, S. Tokonami, H. Nakao, and T. Nagaoka, *Chem. Commun.*, **2009**, 3615.
13. R. Morita, R. Inoue, S. Tokonami, Y. Yamamoto, M. Nakayama, H. Nakao, H. Shiigi, and T. Nagaoka, *J. Electrochem. Soc.*, **158**, K95 (2011).
14. M. D. Musik, C. D. Keating, M. H. Keefe, and M. J. Natan, *Chem. Mater.*, **9**, 1499 (1997).
15. Y. Liu, Y. Wang, and R. O. Claus, *Chem. Phys. Lett.*, **298**, 315 (1998).
16. H. Shiigi, S. Tokonami, H. Yakabe, and T. Nagaoka, *J. Am. Chem. Soc.*, **127**, 3280 (2005).
17. S. Tokonami, H. Shiigi, and T. Nagaoka, *Anal. Chem.*, **80**, 8071 (2008).
18. L. Han, D. R. Daniel, M. M. Maye, and C. J. Zhong, *Anal. Chem.*, **73**, 4441 (2001).
19. I. D. Walton, S. M. Norton, A. Balasingham, L. He, D. F. Oviso, D. Gupta, P. A. Raju, M. J. Natan, and R. G. Freeman, *Anal. Chem.*, **74**, 2240 (2002).
20. C. C. Chen, Y. P. Lin, C. W. Wang, H. C. Tzeng, C. H. Wu, Y. C. Chen, C. P. Chen, L. C. Chen, and Y. C. Wu, *J. Am. Chem. Soc.*, **128**, 3709 (2006).
21. H. Shiigi, Y. Yamamoto, H. Yakabe, S. Tokonami, and T. Nagaoka, *Chem. Commun.*, **2003**, 1038.
22. Y. Yamamoto, N. Yoshi, H. Shiigi, and T. Nagaoka, *Solid State Ionics*, **177**, 2325 (2006).
23. Y. Yamamoto, H. Shiigi, and T. Nagaoka, *Electroanal.*, **17**, 2224 (2005).
24. K. Slowinski, R. V. Chamberlain, C. J. Miller, and M. Majda, *J. Am. Chem. Soc.*, **119**, 119101 (1997).
25. M. A. Rampi and G. M. Whitesides, *Chem. Phys.*, **281**, 373 (2002).
26. M. L. Chabinyc, X. Chen, R. E. Holmlin, H. Jacobs, H. Skulason, C. D. Frisbie, V. Mujica, M. A. Ratner, M. A. Rampi, and G. M. Whitesides, *J. Am. Chem. Soc.*, **124**, 11730 (2002).
27. R. L. York, P. T. Nguyen, and K. Slowinski, *J. Am. Chem. Soc.*, **125**, 5948 (2003).
28. E. A. Weiss, R. C. Chiechi, G. K. Kaufman, J. K. Kriebel, Z. Li, M. Duati, M. A. Rampi, and G. M. Whitesides, *J. Am. Chem. Soc.*, **129**, 4336 (2007).
29. D. J. Wold and C. D. Frisbie, *J. Am. Chem. Soc.*, **122**, 2970 (2000).
30. X. D. Cui, A. Primak, X. Zarate, J. Tomfohr, O. F. Sankey, A. L. Moore, T. A. Moore, D. Gust, G. Harris, and S. M. Lindsay, *Science*, **294**, 571 (2001).
31. B. Q. Xu and N. J. Tao, *Science*, **301**, 1221 (2003).
32. W. Haiss, H. van Zalinge, D. Bethell, J. Ulstrup, D. J. Schiffrin, and R. J. Nichols, *Faraday Discuss.*, **131**, 253 (2006).
33. L. Venkataraman, J. E. Klare, I. W. Tam, C. Nuckolls, M. S. Hybertsen, and M. L. Steigerwald, *Nano Lett.*, **6**, 458 (2006).
34. X. Li, J. He, J. Hihath, B. Xu, S. M. Lindsay, and N. Tao, *J. Am. Chem. Soc.*, **128**, 2135 (2006).
35. Y. Yamamoto, S. Takeda, H. Shiigi, and T. Nagaoka, *J. Electrochem. Soc.*, **154**, D462 (2007).
36. S. Tokonami, Y. Yamamoto, Y. Mizutani, I. Ota, H. Shiigi, and T. Nagaoka, *J. Electrochem. Soc.*, **156**, D558 (2009).
37. S. Tokonami, S. Shirai, I. Ota, N. Shibutani, Y. Yamamoto, H. Shiigi, and T. Nagaoka, *J. Electrochem. Soc.*, **158**, D689 (2011).
38. K. Ogura, H. Shiigi, T. Oho, and T. Tonosaki, *J. Electrochem. Soc.*, **147**, 4351 (2000).
39. R. G. Nuzzo and D. L. Allara, *J. Am. Chem. Soc.*, **105**, 4481 (1983).
40. R. G. Nuzzo, B. R. Zegarski, and L. H. Dubois, *J. Am. Chem. Soc.*, **109**, 733 (1987).
41. A. Ulman, *Chem. Rev.*, **96**, 1533 (1996).
42. F. Schreiber, *Prog. Surf. Sci.*, **65**, 151 (2000).
43. D.-H. Tsai, R. A. Zangmeister, L. F. Pease III, M. J. Tarlov, and M. R. Zachariah, *Langmuir*, **24**, 8483 (2008).
44. M. C. Tan, J. Y. Ying, and G. M. Chow, *J. Mater. Sci. Mater. Med.*, **20**, 2091 (2009).
45. W. Hou, M. Dasog, and R. W. J. Scott, *Langmuir*, **25**, 12954 (2009).
46. H. Qian, Y. Zhu, and R. Jin, *Proc. Natl. Acad. Sci. U.S.A.*, **109**, 696 (2012).
47. C. K. Yee, A. Ulman, J. D. Ruiz, A. Parikh, H. White, and M. Rafailovich, *Langmuir*, **19**, 9450 (2003).
48. R. H. Terrill, T. A. Postlethwaite, C. H. Chen, C. D. Poon, A. Terzis, A. D. Chen, J. E. Hutchison, M. R. Clark, G. Wignall, J. D. Londono, R. Superfine, M. Falvo, C. S. Johnson, E. T. Samulski, and R. W. Murray, *J. Am. Chem. Soc.*, **117**, 12537 (1995).
49. T. Lee, W. Wang, J. F. Klemic, J. J. Zhang, J. Su, and M. A. Reed, *J. Phys. Chem. B*, **108**, 8742 (2004).
50. A. Salomon, D. Cahen, S. Lindsay, J. Tomfohr, V. B. Engelkes, and C. D. Frisbie, *Adv. Mater.*, **15**, 1881 (2003).
51. K. Slowinski, R. V. Chamberlain, R. Bilewicz, and M. Majda, *J. Am. Chem. Soc.*, **118**, 4709 (1996).
52. R. L. York and K. Slowinski, *J. Electroanal. Chem.*, **550-551**, 327 (2003).
53. K. Slowinski and M. Majda, *J. Electroanal. Chem.*, **491**, 139 (2000).
54. K. Slowinski, H. K. Y. Fong, and M. Majda, *J. Am. Chem. Soc.*, **121**, 7257 (1999).
55. S. Sek, R. Bilewicz, and K. Slowinski, *Chem. Commun.*, **2004**, 404.
56. R. E. Holmlin, R. F. Ismagilov, R. Haag, V. Mujica, M. A. Ratner, M. A. Rampi, and G. M. Whitesides, *Angew. Chem., Int. Ed.*, **40**, 2316 (2001).
57. R. E. Holmlin, R. Haag, M. L. Chabinyc, R. F. Ismagilov, A. E. Cohen, A. Terfort, M. A. Rampi, and G. M. Whitesides, *J. Am. Chem. Soc.*, **123**, 5075 (2001).
58. F. P. Zamborini, M. C. Leopold, J. F. Hicks, P. J. Kulesza, M. A. Malik, and R. W. Murray, *J. Am. Chem. Soc.*, **124**, 8958 (2002).